REPORT DOCUMENTATION PAGE

Form Approved OMB NO. 0704-0188

The public reporting burden for this collection of information is estimated to average 1 hour per response, including the time for reviewing instructions, searching existing data sources, gathering and maintaining the data needed, and completing and reviewing the collection of information. Send comments regarding this burden estimate or any other aspect of this collection of information, including suggesstions for reducing this burden, to Washington Headquarters Services, Directorate for Information Operations and Reports, 1215 Jefferson Davis Highway, Suite 1204, Arlington VA, 22202-4302. Respondents should be aware that notwithstanding any other provision of law, no person shall be subject to any oenalty for failing to comply with a collection of information if it does not display a currently valid OMB control number.
PLEASE DO NOT RETURN YOUR FORM TO THE ABOVE ADDRESS.

1. REPORT DATE (DD-MM-YYYY)	2. REPORT TYPE	3. DATES COVERED (From - To)
23-08-2013	Final Report	1-Oct-2012 - 30-Jun-2013

4. TITLE AND SUBTITLE	5a. CONTRACT NUMBER
Stablization of Nanotwinned Microstructures in Stainless Steels Through Alloying and Microstructural Design	W911NF-12-1-0586
	5b. GRANT NUMBER
	5c. PROGRAM ELEMENT NUMBER
	611102

6. AUTHORS	5d. PROJECT NUMBER
Raymundo Arroyave	
	5e. TASK NUMBER
	5f. WORK UNIT NUMBER

7. PERFORMING ORGANIZATION NAMES AND ADDRESSES	8. PERFORMING ORGANIZATION REPORT NUMBER
Texas Engineering Experiment Station Office of Sponsored Research 400 Harvey Mitchell Parkway South, Suite 300 College Station, TX 77845 -4375	

9. SPONSORING/MONITORING AGENCY NAME(S) AND ADDRESS(ES)	10. SPONSOR/MONITOR'S ACRONYM(S)
U.S. Army Research Office P.O. Box 12211 Research Triangle Park, NC 27709-2211	ARO
	11. SPONSOR/MONITOR'S REPORT NUMBER(S)
	62601-MS-II.1

12. DISTRIBUTION AVAILIBILITY STATEMENT

Approved for Public Release; Distribution Unlimited

13. SUPPLEMENTARY NOTES

The views, opinions and/or findings contained in this report are those of the author(s) and should not contrued as an official Department of the Army position, policy or decision, unless so designated by other documentation.

14. ABSTRACT

In this STIR we proposed to investigate the microstructure and alloy composition on the formation and stability of nanotwinned microstructures. The long-term alloy design strategy focuses on microalloying additions to 1) reduce the stacking fault energy (SFE), enhance twinning formation, and increase twin volume fraction; 2) reduce the twin size via increasing interstitial content while also taking into account solid solution hardening in twin size; 3) form high temperature, mainly intergranular, carbides, nitrides, carbonitrides to pin twin boundaries, increasing their

15. SUBJECT TERMS

materials design, stainless steels, plastic deformation by twinning, computational materials science, experimental characterization

16. SECURITY CLASSIFICATION OF:			17. LIMITATION OF ABSTRACT	15. NUMBER OF PAGES	19a. NAME OF RESPONSIBLE PERSON
a. REPORT	b. ABSTRACT	c. THIS PAGE	UU		Raymundo Arroyave
UU	UU	UU			19b. TELEPHONE NUMBER
					979-845-5416

Standard Form 298 (Rev 8/98)
Prescribed by ANSI Std. Z39.18

Report Title

Stablization of Nanotwinned Microstructures in Stainless Steels Through Alloying and Microstructural Design

ABSTRACT

In this STIR we proposed to investigate the microstructure and alloy composition on the formation and stability of nanotwinned microstructures. The long-term alloy design strategy focuses on microalloying additions to 1) reduce the stacking fault energy (SFE), enhance twinning formation, and increase twin volume fraction; 2) reduce the twin size via increasing interstitial content while also taking into account solid solution hardening in twin size; 3) form high temperature, mainly intergranular, carbides, nitrides, carbonitrides to pin twin boundaries, increasing their high temperature stability; 4) form nano-scale intermetallic precipitates in the presence of Co and refractory elements for creep resistance and high temperature strength. Microstructural design strategy would concentrate on twinning-induced grain boundary engineering and distribution of nano-precipitates/carbides.

In the present STIR project focused mainly on the formation and stability of deformation nano-twins in the single crystals of low SFE austenitic stainless steels , experimentally. We did some preliminary investigation on the phase stability of precipitate phases likely to stabilize twinned structure at elevated temperatures. This computational work was accompanied by few experimental validation cases through microstructural investigations and thermo-mechanical testing.   The experimental work was performed in collaboration with Prof. Ibrahim Karaman

Enter List of papers submitted or published that acknowledge ARO support from the start of the project to the date of this printing. List the papers, including journal references, in the following categories:

(a) Papers published in peer-reviewed journals (N/A for none)

Received   Paper

   TOTAL:

Number of Papers published in peer-reviewed journals:

(b) Papers published in non-peer-reviewed journals (N/A for none)

Received   Paper

   TOTAL:

Number of Papers published in non peer-reviewed journals:

(c) Presentations

Number of Presentations: 0.00

Non Peer-Reviewed Conference Proceeding publications (other than abstracts):

Received   Paper

TOTAL:

Number of Non Peer-Reviewed Conference Proceeding publications (other than abstracts):

Peer-Reviewed Conference Proceeding publications (other than abstracts):

Received   Paper

TOTAL:

Number of Peer-Reviewed Conference Proceeding publications (other than abstracts):

(d) Manuscripts

Received   Paper

TOTAL:

Number of Manuscripts:

Books

Received   Paper

TOTAL:

Patents Submitted

Patents Awarded

Awards

Graduate Students

NAME	PERCENT_SUPPORTED	Discipline
Shengyen Li	0.25	
Taymaz Jozaghi	0.25	
Chung J. Wang	0.25	
Ruixian Zhu	0.25	
FTE Equivalent:	**1.00**	
Total Number:	**4**	

Names of Post Doctorates

NAME	PERCENT_SUPPORTED
FTE Equivalent:	
Total Number:	

Names of Faculty Supported

NAME	PERCENT_SUPPORTED	National Academy Member
Raymundo Arroyave	0.10	
Ibrahim Karaman	0.00	
FTE Equivalent:	**0.10**	
Total Number:	**2**	

Names of Under Graduate students supported

NAME	PERCENT_SUPPORTED
FTE Equivalent:	
Total Number:	

Student Metrics

This section only applies to graduating undergraduates supported by this agreement in this reporting period

The number of undergraduates funded by this agreement who graduated during this period: 0.00

The number of undergraduates funded by this agreement who graduated during this period with a degree in science, mathematics, engineering, or technology fields:...... 0.00

The number of undergraduates funded by your agreement who graduated during this period and will continue to pursue a graduate or Ph.D. degree in science, mathematics, engineering, or technology fields:...... 0.00

Number of graduating undergraduates who achieved a 3.5 GPA to 4.0 (4.0 max scale): 0.00

Number of graduating undergraduates funded by a DoD funded Center of Excellence grant for Education, Research and Engineering:...... 0.00

The number of undergraduates funded by your agreement who graduated during this period and intend to work for the Department of Defense 0.00

The number of undergraduates funded by your agreement who graduated during this period and will receive scholarships or fellowships for further studies in science, mathematics, engineering or technology fields: 0.00

Names of Personnel receiving masters degrees

NAME

Total Number:

Names of personnel receiving PHDs

NAME
Shengyen Li
Ruixian Zhu

Total Number: 2

Names of other research staff

NAME	PERCENT_SUPPORTED

FTE Equivalent:
Total Number:

Sub Contractors (DD882)

Inventions (DD882)

Scientific Progress

Technology Transfer

Stablization of Nanotwinned Microstructures in Stainless Steels Through Alloying and Microstructural Design

FINAL REPORT

For the Period:
October 1st, 2012 to June 30ᵗʰ, 2013
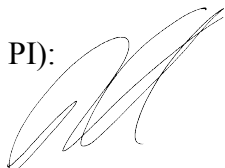
to
U.S. Army – Army Research Office

On the Award No.
W911NF-12-1-0586 - TEES
Program Officer: Dr. Suveen N. Mathaudhu

Date of Submission: August 22ⁿᵈ, 2013

Principal Investigator
Raymundo Arroyave
Associate Professor
Department of Materials Science and Engineering
Texas A&M University, Texas A&M Engineering Experiment Station
College Station, TX
Email: rarroyave@tamu.edu
Phone: 979-845-5416

Recipient Organization:
Texas Engineering Experiment Station
DUNS: 84-720-5572

Signature of Submitting Official (the PI):

Table of Contents

Stablization of Nanotwinned Microstructures in Stainless Steels Through Alloying and Microstructural Design

Raymundo Arroyave, Texas A&M University

1   Preamble

One of the most significant challenges for the development of high-performance structural materials is the de-stabilization of optimized microstructures when operating at relatively high homologous temperatures. While this problem is especially pressing in areas of power generation and aerospace propulsion, the problem of stabilization of nano-structures is highly relevant to many other applications of interest to ARO. In this STIR we focused on the generation—through thermo-mechanical processing--- and stabilization—through alloying and nano-precipitate engineering---of nanotwinned stainless steels. This preliminary work has provided valuable insight into the mechanisms responsible for the stabilization of a wider class of nanotwinned materials. Knowledge gained from this program is currently being used to develop guidelines for the design of stable nanotwinned microstructures.
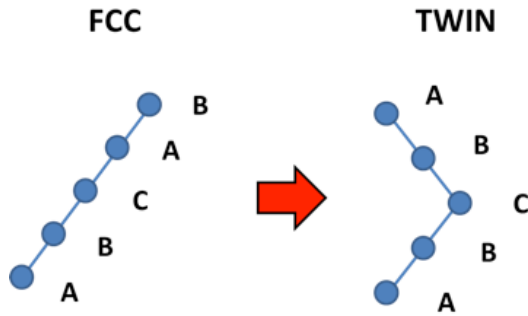
The microstructure design will exploit nano-twinning-induced grain boundary engineeringstrategies which will target high density of low energy grain and nano-twin boundaries, pinned by nano-scale precipitates - formed at very high temperatures- for high-temperature strength and stability. The *uniqueness* of the proposed approach originates from the synergistic combination of computational alloy design expertise with microstructural design and thermo-mechanical processing capabilities for accelerated discovery of the next generation advanced high temperature stainless steels.

2   Research Activities

In this STIR we proposed to investigate the microstructure and alloy composition on the formation and stability of nanotwinned microstructures. The long-term alloy design strategy focuses on microalloying additions to 1) reduce the stacking fault energy (SFE), enhance twinning formation, and increase twin volume fraction; 2) reduce the twin size via increasing interstitial content while also taking into account solid solution hardening in twin size; 3) form high temperature, mainly intergranular, carbides, nitrides, carbonitrides to pin twin boundaries, increasing their high temperature stability; 4) form nano-scale intermetallic precipitates in the presence of Co and refractory elements for creep resistance and high temperature strength. Microstructural design strategy would concentrate on twinning-induced grain boundary engineering and distribution of nano-precipitates/carbides. The work would also involve a fundamental study on the thermal stability of deformation nano-twins at high temperatures and their influence on the recovery/recrystallization of austenitic stainless steels.

In the present STIR project **focused mainly** on the formation and stability of deformation nano-twins in the single crystals of low SFE austenitic stainless steels , experimentally. We did some preliminary investigation on the phase stability of precipitate phases likely to stabilize twinned structure at elevated temperatures. This computational work was accompanied by few experimental validation cases through microstructural investigations and thermo-mechanical testing. The experimental work was performed in collaboration with Prof. Ibrahim Karaman.

2.1 Fundamental Investigations on Twinning Behavior in Fe-based Alloy Systems

Figure 1: Schematic diagram of twining in fcc systems.

The likely operative deformation mechanism of the steel alloys can be understood in part by examining the behavior stacking fault energy (SFE), which is generally defined as the deformation characteristics and mechanical behavior of the materials. In a simple-minded way, from low to high SFE, the plastic deformation of steel alloys can be divided into three preferred stages: (1) martensitic transformation, (2) twinning and gliding and (3) gliding [1-3]. This means, that with lower SFE, the alloy possesses higher tendency to twin in FCC phase. Although there have been a great number of experimental and theoretical investigations on the intrinsic factors that control the SFE, many questions remain. This is particularly true when considering that one of the major goals of the present project were to incorporate a metric for twinnability in the overall alloy design scheme.

From a thermodynamic point of view, twinning in fcc systems corresponds to a local phase transition where the normal ABC stacking is locally transformed to a AB stacking corresponding to an hcp crystal structure. Thus, to a first approximation, SFE can in principle be expressed as a function of molar surface density, molar Gibbs free energy change during the phase transformation (in this case, fcc to hcp), and surface energy of the interface ($\gamma = 2\rho\Delta G + 2\sigma$). Thermodynamics models have been built to estimate the required free energy change for the local fcc to hcp transformation (essentially a martensitic transition). From these models, it has been concluded that by adding Ni, Al and Cu, SFE goes higher; whereas by adding Cr, SFE decreases [3, 5]. This indicates the importance of the chemical composition.

Another important issue is the criterion to increase the twinning density. Twinnability is the quantity characterizing the ability of a material to deform through twinning deformation [6]. This quantity can also be expressed as a function of the unstable stacking energy (USE) and unstable twinning energy (UTE). From first principle calculations, these two properties can be evaluated.
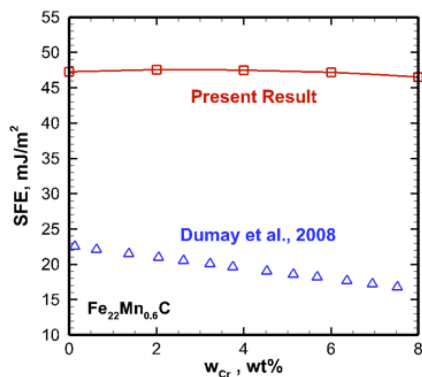

Figure 2: The SFE calculated by the thermodynamic model comparing to the experimental results[4]

This model provides the qualitatively results comparing to the experiments.

Thermodynamic Approach

The stacking fault energy (SFE) in austenitic stainless steel can be estimated using either thermodynamic models or first-principle calculations. In this work the thermodynamic database, TCFE6 V6.2, is utilized to calculated the SFE with the model [4, 7]

$$\Gamma = 2.88 \times 10^{-5} \Delta G^{\gamma \to \varepsilon} + 16 \ (mJ \cdot mol^{-1})$$

where 16 $mJ \cdot mol^{-1}$ represents the interfacial energy of the twinning. To evaluate this model, we attempted to compare the experimental results on $Fe_{22}Mn_{0.6}C$ based alloy with various Cr content

performed by Dumay and collaborators [4] with the results obtained from the thermodynamic approach. As shown in **Fig. 2** there is a discrepancy between the calculation using TCFE6 (V6.2) and the published results. Our model calculations overestimate the SFE in the alloy system by a factor of two. While the reason for the discrepancy is not clear at the moment, it is likely that the major contributor is the fact that the free energy differences between fcc and hcp according to the thermodynamic database are overestimated. This is likely to the fact that the Fe-rich hcp phase has not been fully assessed. This is in part due to the scarce thermodynamic and phase equilibria data where hcp-Fe is a relevant phase. Given the fact that this quantity (difference in energy between fcc and hcp) is not easily accessible experimentally, we proceeded to investigate the use of DFT calculations to estimate SFE.

Density Functional Theory Calculations

The fcc-hcp martensitic transformation is presented from atomic point of view in **Fig. 3**. The initial atomic arrangement is in sequence of ABCABCA and transformed into ABCACAB with respect to the inhabit plane of atom A [8]. It also represents the model for calculating the intrinsic stacking fault as a function of the difference in energy between the faulted and perfect crystal structure, and the specific surface area of the plan parallel to the fault [9]:

$$\Gamma = \frac{F_{SF} - F_0}{A_{2D}}$$
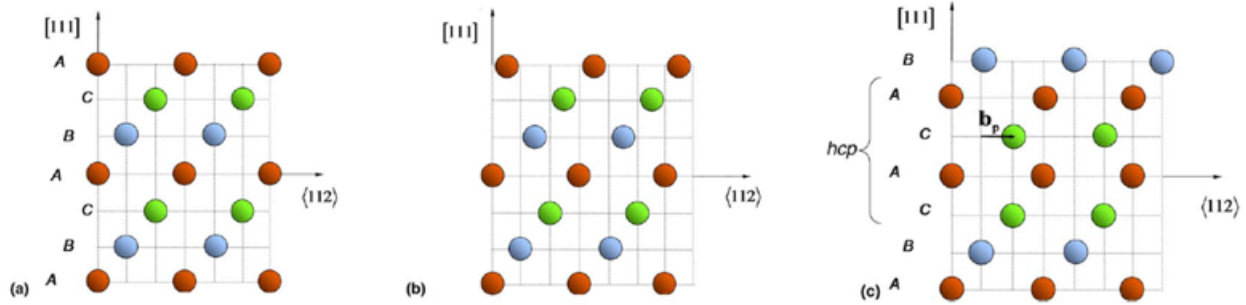
Figure 3: The schematic process of the martensitic transformation [8]

While the calculation of the quantity above can be routinely done using first principles approaches, other approximations can be made in order to facilitate the rapid estimation of SFE within minimum computational effort. According to the Axial Next-Nearest-Neighbour Ising (ANNNI) model, the total energy of a system with different sacking sequences can be represented as [9]:

$$E = E_0 - J_1 \sum_i S_i S_{i+1} - J_2 \sum_i S_i S_{i+2} - J_3 \sum_i S_i S_{i+3}$$

The energy different of the stacking fault can therefore be estimated based on the free energies of the HCP and FCC phases in a first order approximation [10, 11]

$$F_{SF} - F_0 = -4J_1 - O(J_2) \approx F_{HCP} - F_{FCC}$$

This model has been utilized to study the effects of substitutional [10, 12, 13] and interstitial [8, 14] elements to SFE of the austenitic stainless steels. Also, the finite temperature model is implemented for practical applications [15, 16]. While this method is rather trivial to implement in conventional DFT codes, the fact that alloys can only be simulated through the use of supercells makes the calculation of the difference in energy as a function of alloy composition

problematic. In order to overcome this limitation, we have examined two alloys, $Fe_{74.5}Cr_{13.5}Ni_{12}$ and $Fe_{70.5}Cr_{17.5}Ni_{12}$, using the EMTO-CPA method[17]. **Fig. 4** shows the optimum wigner-seitz radii of FCC and HCP phases of these two alloys and the SFEs are calculated accordingly as shown in **Fig. 4**. Comparing to the work by Vitos et al. [11], the calculations present reasonable results.
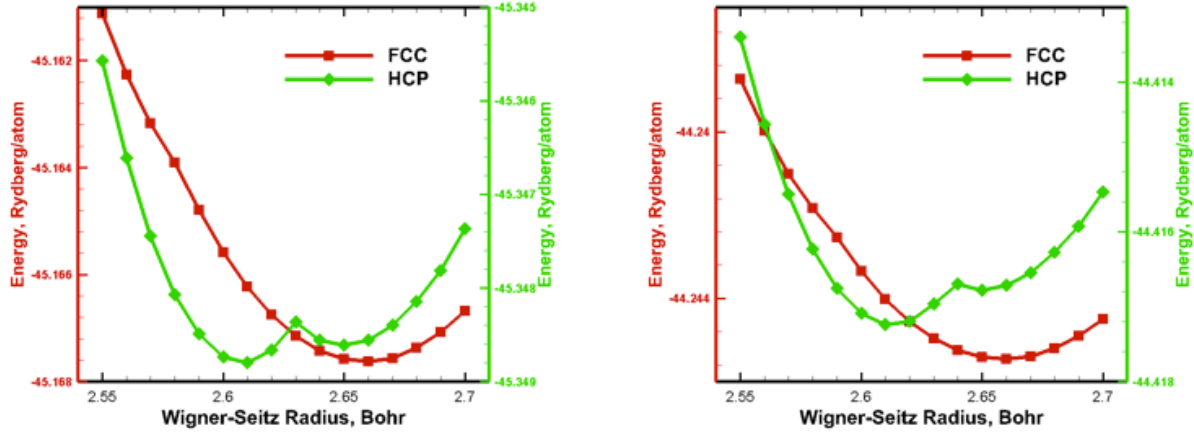
**Figure 4:** The stability of the FCC and HCP phases of $Fe_{74.5}Cr_{13.5}Ni_{12}$ and $Fe_{70.5}Cr_{17.5}Ni_{12}$

Table 1. The calculated energy states and SFE; μ stands the magnetic moment (average of Fe and Mn) of FCC and HCP (μ_B); γ_0, $\gamma_{M,RT}$, γ are the stacking fault energies (mJ/m^2) at 0 Kelvin, affected by magnetic moment contributions to entropy at room temperature and total SFE at room temperature.

|	μ^{FCC}	μ^{HCP}	γ_0	$\gamma_{M,RT}$	γ
$Fe_{74.5}Cr_{13.5}Ni_{12}$	1.61	0.00	7.03	30.71	37.75
[14]	1.62	0.00	8.50	36.20	44.60
$Fe_{70.5}Cr_{17.5}Ni_{12}$	1.54	0.00	6.67	29.84	36.51
[14]	1.54	0.00	-1.10	29.70	28.60
$Fe65.5Cr_{17.5}Ni_{12}Mn_5$	1.32	0.00	7.19	26.97	34.15

The results shown in **Table 1** are worth further examination: as can be seen from the table, the 0K stacking fault energy calculated at 0K is rather law. Moreover, it can be seen how different the magnetization is between fcc and hcp. This means that magnetic properties are likely to play a major role due to their contribution to the entropy differences---and free energy differences. In fact, the table shows that magnetic contributions can account for more than 75% of the stacking fault energy in Fe-based compositions close to those of typical stainless steels.

In order to further investigate the twinning deformation behavior in Fe-based fcc alloys, we proceeded to investigate the Generalized Stacking Fault Energy surface according to the method proposed by Janhatek and collaborators[18]. The methodology allows for the investigation of shearing deformation parallel to the (111) planes along different important directions, [11-2] and [-110] (**Fig. 5a**). Two different types of deformations—affine and alias—have been investigated. Under an affine shear deformation, all atoms are shifted parallel to the shearing direction by a distance proportional to their distance from the fixed basal plane. In the alias regime, only the top layer is displaced in the shearing direction. **Fig. 5b** contains a schematic of the deformation
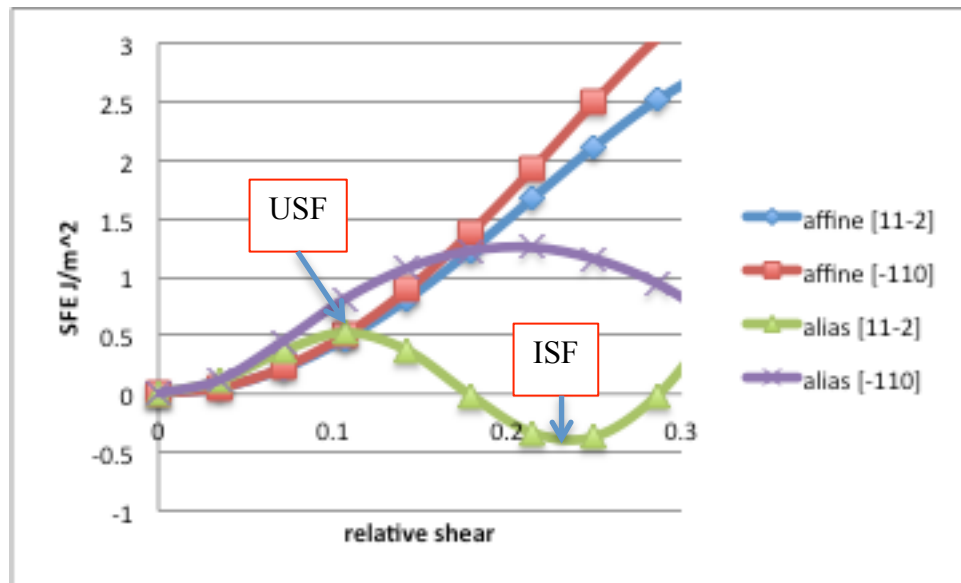
mechanism considered in this work.
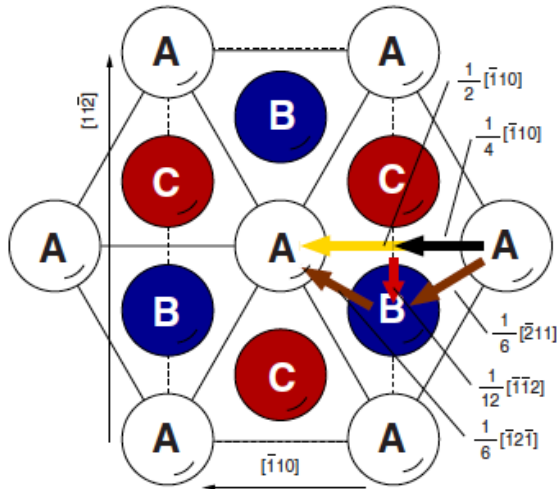
**Figure 5a:** Geometry of shear deformation on (111) planes[18].
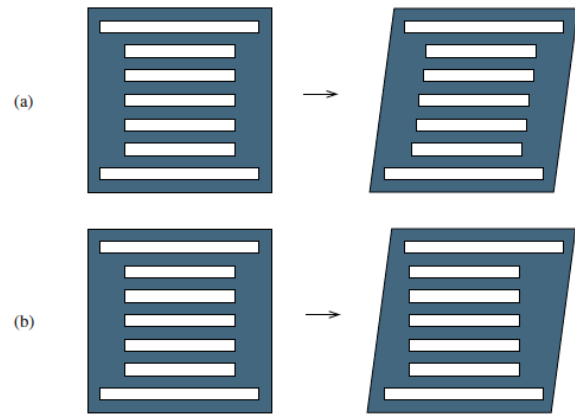
Figure 5b: The schematic view of possible deformation regimes: **(a)** affine shear, **(b)** the alias shear[18].

Figure 6: Generalized stacking fault energy surface for pure Fe, without considering magnetism. Green curve corresponds to fcc-hcp transformation under alias shear. Calculations were done at 0K.

Fig . 6 shows the Generalized Stacking Fault Energy (GFSE) surface for Fe along the [11-2] and [-110] directions under alias and affine shears. The curve corresponding to the alias shear along the [11-2] direction corresponds to the conventional deformation driving the transformation from fcc to hcp. This curve shows that the SFE is actually negative at the absolute minimum of the transformation path. This point corresponds to the Intrinsic Stacking Fault. The negative value means that the structure is unstable against this deformation. This makes sense as the hcp structure in Fe when no spin magnetization is considered is actually more stable than fcc

7

Fe.
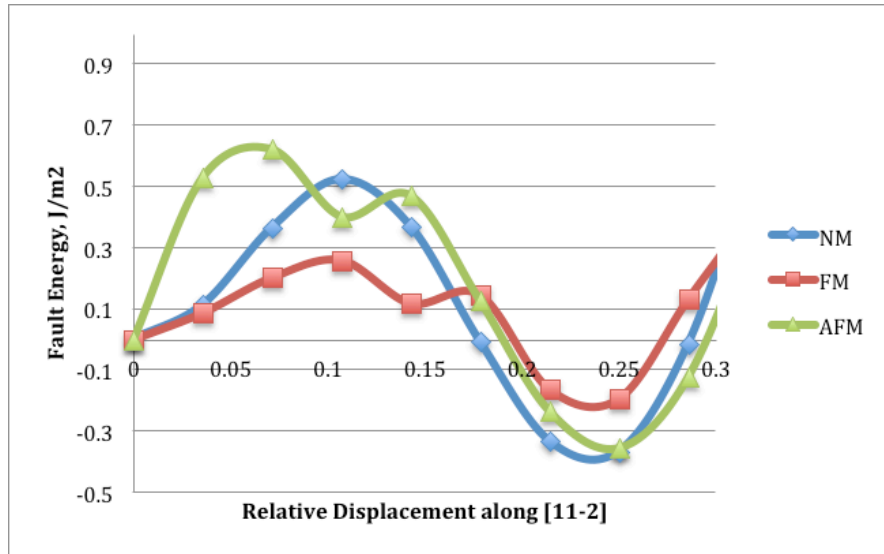
Figure 7: Generalized stacking fault energy (GSFE) surface for pure Fe along the [11-2] direction considering different magnetic states at 0K.

Fig. 7 shows similar calculations as shown in **Fig. 6**, comparing different magnetic states in fcc Fe: NM (non magnetic), FM (anti-ferromagnetic) and AFM (anti-ferromagnetic). Here it is important to note that the actual magnetic state for fcc Fe is more complex than the configurations considered. However, it is important to note that regardless of the state, hcp is still more stable than fcc. Note, however, that in the case of AFM state, the barrier necessary to overcome in order for the transformation to occur is actually higher than in the NM state. Note also how a FM arrangement leads to a less stable hcp. Note also that in this case no contributions due to entropy have been taken into account. It is likely that these effects are sufficient to raise the GFSE curve, although it is unlikely that the ISF reaches positive values under the approximations considered.

Future work along the lines outlined above will consist of including all possible contributions to the free energy of the GFSE surface. Moreover, alloying effects will be considered.

2.2 Plastic Deformation Mechanisms in 316 Stainless Steels

To help the alloy design by providing better understanding of microstructural evolutions through microstructural characterization, single crystals of stainless steel 316 were fabricated to study the effect of mechanical deformation on twin formation and the changes in the twin structure during recovery and recrystallization. Single crystals were grown using the Bridgman technique in He and were then cut into dog-bone shape tensile samples with the gage dimensions of 8 mm x 3mm x 1mm using wire electro discharge machining.

316 single crystals with composition shown in **Table 2** were used for tension test at room temperature and -80°C. The elemental composition table was provided using EDS analysis and, therefore, may include a ±5 wt% error. Nitrogen was added to this composition to study its effect on twin-ability of stainless steel 316L and forming possible nitro-carbides.

Table 2. Composition of 316LN single crystals from EDS analysis

Element	C	N	Cr	Cu	Mn	Mo	Ni	O	P	S	Si	Fe
wt%	0.08	0.20	17.73	0.25	1.07	2.26	11.78	0.0012	0.014	0.014	0.44	bal.

316 [111] single crystals were cut into dog bone-shaped specimens and were heat treated for 12 hours at 1080°C, then at 1100°C for 1 hour and consequently water quenched, in order to homogenize the microstructure. One sample was then used in uniaxial tension test for 20% deformation at room temperature (**Fig. 8a**). EBSD results of this sample are shown in **Fig. 8b**. The results show that a twinning texture of {111}/{112} exists, and the band of the twins vary from less than 1μm to larger than 40μm.
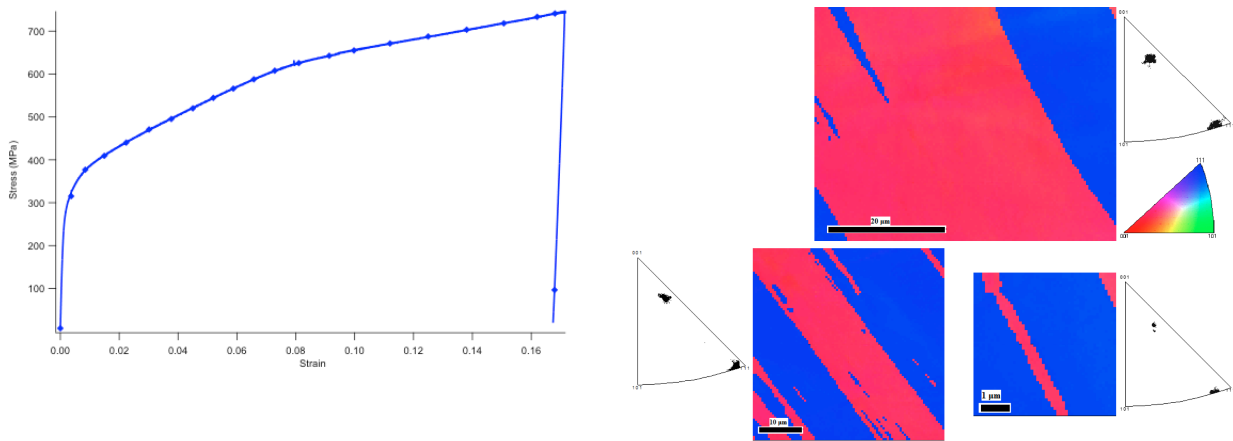
Figure 8: (a) Strain-Stress behavior of 316 [111] crystal sample uniaxial tension test at room temperature (b) EBSD analysis of 316 [111] single crystals deformed to 20% at room temperature.
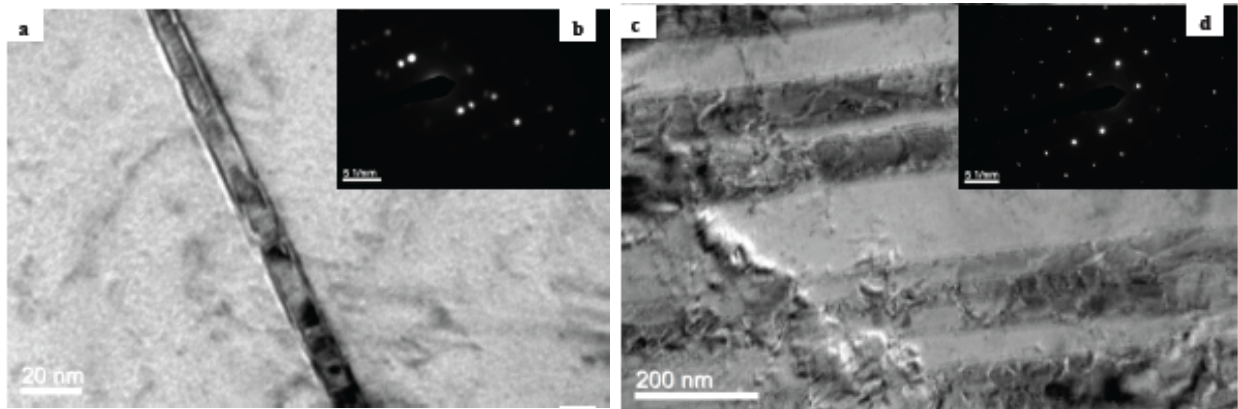

Figure 9: TEM images of 20% deformed 316 [111] single crystal samples

The 20% deformed 316 [111] single crystal samples was studied using TEM. **Fig. 9** shows two TEM images of this sample. In **Fig. 9-a**, a 10nm wide band can be detected, and **Fig. 9-b** shows the diffraction, indicating that this is twinning. Also **Error! Reference source not found.9-c** shows another set of bands, around 100nm wide, with the corresponding diffraction pattern in **Fig. 9-d** it is suggested that these bands may be stacking faults. These TEM and EBSD results are promising and investigation will continue on optimizing the twin size and its interaction with precipitates, as well as other mechanical properties at room temperature and high temperature

2.3 Phase Stability in Stainless Steels

As mentioned above, the formation of nano-size precipitates is beneficial to stabilize nanotwinned microstructure at elevated temperatures. It is recently shown in 316 stainless and Fe-Mn austenitic steels that nano-carbides prefer forming at grain boundaries and faults [19-21] and that these phase can stabilize nanostructures and improve properties at elevated temperatures[22, 23]. However, one problem is to control the temperature at which these carbides form. Low temperature carbides/nitrides should be suppressed such that the microstructure is stable during long high temperature exposure. To achieve this, we have considered using elements such as Si (to a certain extent not to form sigma phase) and Al, and/or forming strong substitutional - interstitial couples with elements such as Mn. Formation of nano-precipitates of MX (M=Nb or W, X = N or C) at very high temperatures can suppress the precipitation of other phases at lower temperatures [24], enhancing the high temperature stability and creep resistance of austenitic stainless steels at desired operating temperatures. Addition of W, Ta, and Nb should also provide significant solid-solution strengthening in the proposed steels.
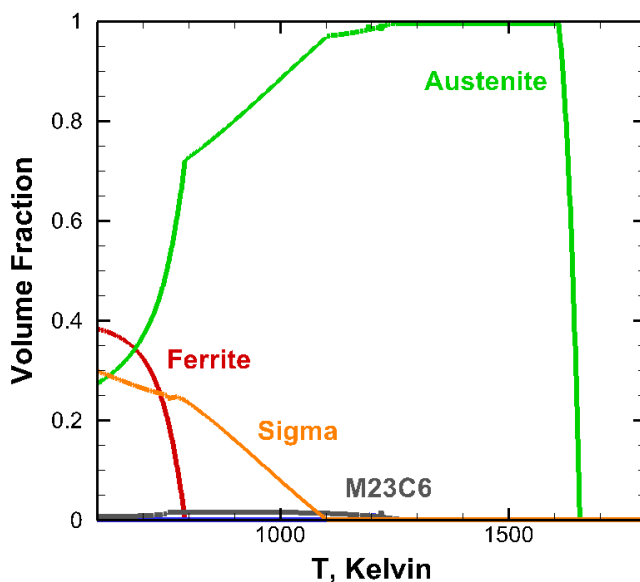
Figure 10: Phase analysis for Stainless Steel 316 with composition shown in **Table 1.**

Based on the composition for Stainless Steel 316 (shown in **Table 1)**, the equilibrium phases are analyzed and shown in **Fig. 10**, according to the TCFE6 V6.2 database, where Sigma phase is the FeCr inter-metallic compound. It indicates that the Laves phase is not stable in this alloy at temperatures higher than 600K. In order to suppress the formation of $M_{23}C_6$, Nb and Ti are added to 316 , as alloy 2 and 3, to form Fe(Nb, Ti)C. The effect of temperature and weight percent of Ti and W on the formation of ferrite (BCC), austenite (FCC), Laves phases, and NbTi carbide is shown in **Fig. 11.**

(a)

(b)
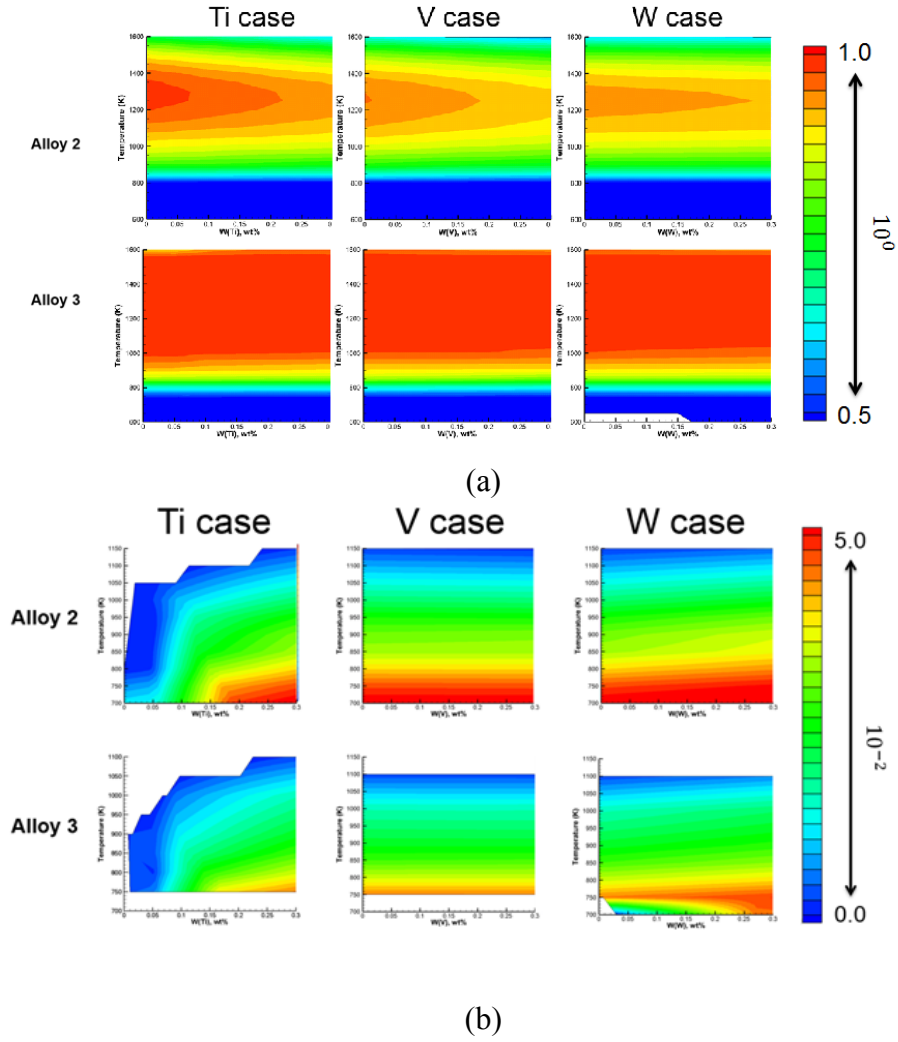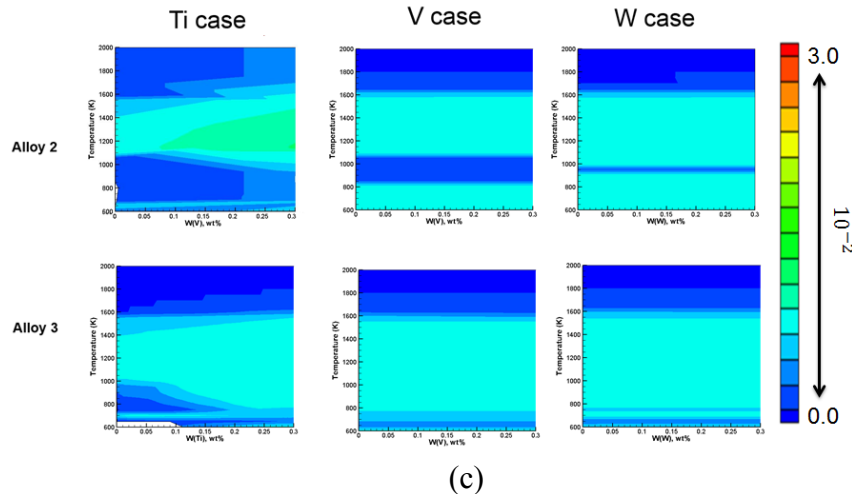
(c)

Figure 11: The effect of Ti and W additions on the volume fraction of (a) Austenite (FCC), (b) Laves Phase, and (c) TiNbC.

It can be observed that the Ti is most effective to stabilize Austenite and TiNbC but it is not as important as V to Laves phase. These contour plots can be utilized for selecting the alloy and, more importantly, for defining the domain of the material optimization. In future work, we will incorporate other elements and we will examine the stability of other possible stabilizing nano-phases, including intermetallic compounds (such as aluminides).

3   Outlook

The **ultimate goal** of this preliminary project was to understand the effects of alloying and microstructure design---through thermo-mechanical processing---on the size, density and stability of nanotwins in stainless steels. This STIR forms the basis of a longer-term program aimed at the design of new austenitic stainless steels with ultrahigh strength, ductility and---as a result of the stable nanotwinned microstructure---high-temperature strength. The long-term goal of this effort is to develop austenitic stainless steels capable of operating at temperatures up to 850^0C that demonstrate yield strength levels on the order of more than a GPa, ultimate tensile strengths (UTS) of more than 2 GPa, and specific strength of more 250 kNm/kg at ambient temperature.

4   References

[1]   Soulami A, Choi KS, Shen YF, Liu WN, Sun X, Khaleel MA. *On deformation twinning in a 17.5% Mn–TWIP steel: A physically based phenomenological model*, Materials Science and Engineering: A 2011;528:1402.
[2]   Hamada AS, Karjalainen LP. *Hot ductility behaviour of high-Mn TWIP steels*, Materials Science and Engineering: A 2011;528:1819.
[3]   Allain S, Chateau JP, Bouaziz O, Migot S, Guelton N. *Correlations between the calculated stacking fault energy and the plasticity mechanisms in Fe–Mn–C alloys*, Materials Science and Engineering: A 2004;387–389:158.
[4]   Dumay A, Chateau J-P, Allain S, Migot S, Bouaziz O. *Influence of addition elements on*

the stacking-fault energy and mechanical properties of an austenitic Fe–Mn–C steel, Materials Science and Engineering: A 2008;483:184.

[5]   Ferreira PJ, Müllner P. *A thermodynamic model for the stacking-fault energy*, Acta Materialia 1998;46:4479.

[6]   Tadmor EB, Bernstein N. *A first-principles measure for the twinnability of FCC metals*, Journal of the Mechanics and Physics of Solids 2004;52:2507.

[7]   Curtze S, Kuokkala V-T, Oikari A, Talonen J, Hänninen H. *Thermodynamic modeling of the stacking fault energy of austenitic steels*, Acta Materialia 2011;59:1068.

[8]   Kibey S, Liu J, Curtis M, Johnson D, Sehitoglu H. *Effect of nitrogen on generalized stacking fault energy and stacking fault widths in high nitrogen steels*, Acta Materialia 2006;54:2991.

[9]   Denteneer P, van Haeringen W. *Stacking-fault energies in semiconductors from first-principles calculations*, Journal of Physics C: Solid State Physics 1987;20:L883.

[10]   Gebhardt T, Music D, Ekholm M, Abrikosov I, Vitos L, Dick A, Hickel T, Neugebauer J, Schneider J. *The influence of additions of Al and Si on the lattice stability of fcc and hcp Fe–Mn random alloys*, Journal of Physics: Condensed Matter 2011;23:246003.

[11]   Vitos L, Nilsson J-O, Johansson B. *Alloying effects on the stacking fault energy in austenitic stainless steels from first-principles theory*, Acta Materialia 2006;54:3821.

[12]   Vitos L, Korzhavyi PA, Johansson B. *Modeling of alloy steels*, Materials Today 2002;5:14.

[13]   Vitos L, Korzhavyi PA, Nilsson J, Johansson B. *Stacking fault energy and magnetism in austenitic stainless steels*, Physica Scripta 2008;77:065703.

[14]   Abbasi A, Dick A, Hickel T, Neugebauer J. *First-principles investigation of the effect of carbon on the stacking fault energy of Fe–C alloys*, Acta Materialia 2011;59:3041.

[15]   Vitos L, Korzhavyi PA, Johansson B. *Evidence of large magnetostructural effects in austenitic stainless steels*, Physical review letters 2006;96:117210.

[16]   Hickel T, Grabowski B, Körmann F, Neugebauer J. *Advancing density functional theory to finite temperatures: methods and applications in steel design*, Journal of Physics: Condensed Matter 2012;24:053202.

[17]   Vitos L. Computational Quantum Mechanics for Materials Engineers: The EMTO Method and Applications: Springer, 2007.

[18]   Jahnátek M, Hafner J, Krajčí M. *Shear deformation, ideal strength, and stacking fault formation of fcc metals: A density-functional study of Al and Cu*, Physical Review B 2009;79:224103.

[19]   Trillo E, Murr L. *Effects of carbon content, deformation, and interfacial energetics on carbide precipitation and corrosion sensitization in 304 stainless steel*, Acta Materialia 1998;47:235.

[20]   Jones R, Randle V. *Sensitisation behaviour of grain boundary engineered austenitic stainless steel*, Materials Science and Engineering: A 2010;527:4275.

[21]   Jones R, Randle V, Owen G. *Carbide precipitation and grain boundary plane selection in overaged type 316 austenitic stainless steel*, Materials Science and Engineering: A 2008;496:256.

[22]   Yamamoto Y, Brady MP, Lu ZP, Liu CT, Takeyama M, Maziasz PJ, Pint BA. *Alumina-Forming Austenitic Stainless Steels Strengthened by LAves Phase and MC Carbide Precipitates*, Metallurgical and Materials Transactions A 2007;38:2737.

[23]   Yamamoto Y, Santella ML, Brady MP, Bei H, Maziasz PJ. *Effect of Alloying Additions*

on Phase Equilibria and Creep Resistance of Alumina-Forming Austenitic Stainless Steels, Metallurgical and Materials Transactions A 2009;40.

[24]   Kim YU, Kwun SI, Shim JH, Park DB, Cho YW, Chung YH, Jung WS. 3rd Symposium on Heat Resistant Steels and Alloys for High Efficiency USC Power Plants. Tsukuba, Japan, 2009.